

Optical tomography of photon-added coherent states, even and odd coherent states, and thermal states

Ya. A. Korennoy and V. I. Man'ko

P.N. Lebedev Physical Institute, Leninsky prospect 53, 117924 Moscow, Russia

(Received 9 February 2011; published 11 May 2011)

Explicit expressions for optical tomograms of photon-added coherent states, even and odd photon-added coherent states, and photon-added thermal states are given in terms of Hermite polynomials. Suggestions for experimental homodyne detection of the considered photon states are presented.

DOI: [10.1103/PhysRevA.83.053817](https://doi.org/10.1103/PhysRevA.83.053817)

PACS number(s): 42.50.Ar, 03.65.Wj, 42.50.Xa, 03.65.Ta

I. INTRODUCTION

Various kinds of nonclassical photon states have been studied during the past two decades (see, e.g., the review [1]). Among the nonclassical states are the so-called photon-added and photon-subtracted states [2].

These states were considered in [3–5]. In [6] it was shown that in photon-subtracted states the mean number of photons may be either less than or greater than that of the initial state, depending on the photon statistics, while in photon-added states the mean number of photons is always greater than that of the initial state. These states were studied experimentally in [7–11], where the commutation relation between bosonic annihilation and creation operators was considered. Experiments were done using homodyne detection of photon states in [12,13] to reconstruct the Wigner function of the photon states. On the other hand the optical tomogram of a quantum state can be considered as a primary object which contains complete information on the quantum state and can serve as an alternative to the density matrix [14,15]. In view of this, homodyne detection used in experiments with photon-added states is of interest per se. Homodyne detection provides, as experimental output, an optical tomogram, which is a fair probability distribution of homodyne quadrature X , depending on an extra parameter θ . This angle parameter is the so-called local oscillator phase, a controlled parameter varying in the domain $0 \geq \theta \geq 2\pi$. Note that this probability satisfies the symmetry relation $w(X, \theta + \pi) = w(-X, \theta)$, and thus in the range $0 \geq \theta \geq \pi$ it completely describes the quantum state [see Eq. (7)].

In [7] the authors used conditional stimulated parametric down-conversion in a nonlinear optical crystal for the production of photon-added states. Here one high-energy pump photon can annihilate into two photons that obey global energy and momentum conservation laws and are normally emitted in symmetrically oriented directions (signal and idler modes). To generate a photon-added state one has to inject a seed (initial) state into a signal mode of the parametric amplifier. The conditional preparation of the target photon-added state will take place every time a single photon is detected in the correlated idler mode.

The primary light source for the experiment is a mode-locked laser whose pulses are frequency-doubled to become the pump for degenerate parametric down-conversion in a type-I beta-barium borate crystal.

The Wigner functions of single photon-added coherent states were reconstructed for experimentally measured data

for $|\alpha| = 0.03, 0.9$, and 2.6 , where $|\alpha|^2$ is the average photon number of the initial coherent state $|\alpha\rangle$ to which a photon is added.

In [8] the authors probed quantum commutation rules by the addition to and subtraction from a light field of single photons. They used the same procedure to generate photon-added, photon-subtracted, photon-added-then-subtracted, and photon-subtracted-then-added states, which are different from one another and from the original seed thermal state. They experimentally measured the quadrature distribution function of photon-added and photon-subtracted states for an initial thermal state with a mean number of photons $\bar{n} = 0.57$. Note that this measured distribution function coincides with the optical tomogram because the density matrix of this state exhibits no phase dependence. In a development of this work [10] the authors measured tomograms of superpositions of photon-added-then-subtracted and photon-subtracted-then-added states, depending on the phase between these two states.

In [9] parametric down-conversion in a nonlinear crystal was used to generate photon-added coherent states, and the non-Gaussianity of these states was investigated. Experimental Wigner functions were reconstructed for single-photon coherent states with $|\alpha| = 0, 0.48$, and 1.02 .

In [11] experimental preparation of single photon-added thermal states and reconstruction of the Glauber-Sudarshan quasiprobability (P function) for these states were carried out.

It has been shown [16] that higher-order photon-added coherent states $|\alpha, m\rangle$ corresponding to $m > 1$ can also be achieved in the parametric down-conversion scheme.

Generation of photon-added coherent states is also possible in the atom-cavity interaction [2].

Moreover, interaction in optomechanical systems (microresonators interacting with laser light) can by proper detuning be used to generate photon-added coherent states in the optomechanical domain [17].

A common feature of the aforementioned experimental techniques is that they all use interacting bipartite systems. During their evolution, the two subsystems are entangled. This enables one to make suitable conditional measurements on one of the subsystems so that the other subsystem is prepared in a photon-added state.

In [18] a comparative study was presented of two processes, namely parametric down-conversion and the atom-cavity interaction, that can generate photon-added states. By expressing the time-evolved states in a suitable nonorthogonal basis, it was established that the former method generates ideal

photon-added states, a feature that is not present in the atom-cavity scheme. Further, parametric down-conversion itself was shown to be capable of generating an ideal m -photon-added state, without requiring higher-order processes.

The aim of this work is to study the optical tomograms of various photon-added nonclassical states. We consider photon-added coherent states, even and odd coherent states [19], and thermal states. The optical tomograms calculated in this paper can be compared with the results of homodyne detection of the photon states, i.e., the output experimental optical tomograms (e.g., in [7–10]). It is worth noting that some recent studies of photon-added states are presented in [18].

We also want to point out that aspects of tomographic probability representation of photon states and of analysis of the precision of the experimentally obtained optical tomograms [7–11] have to be discussed in connection with other experiments where various photon states were studied; see, e.g., [20].

In the published results, not all the tests associated with the uncertainty relations and the dependence of the optical tomogram on local oscillator phase have been given in detail and in explicit form. Another goal of our work is to suggest that more attention be paid to the variety of possible tests, which permits better accuracy in the measurement of such primary objects as optical tomograms identified with quantum states.

The paper is organized as follows. In Sec. II a short review of the optical tomographic representation of photon states is given. In Sec. III we review a model of a parametric oscillator, and photon-added states appearing in this model are considered. A summary of results is presented in Sec. IV.

II. OPTICAL TOMOGRAPHIC REPRESENTATION

In this section we review the tomographic probability representation of quantum states [15]. Given a density operator $\hat{\rho}$ (one-mode photon state), the symplectic tomogram $M(X, \mu, \nu)$, which is the normalized probability distribution of homodyne quadrature X depending on two real parameters μ and ν , is defined as

$$M(X, \mu, \nu) = \text{Tr}[\hat{\rho}\delta(X - \mu\hat{q} - \nu\hat{p})] = \langle X, \mu, \nu | \hat{\rho} | X, \mu, \nu \rangle, \quad (1)$$

where \hat{q} and \hat{p} are operators of the first and second photon quadratures, and $|X, \mu, \nu\rangle$ is an eigenvector of the Hermitian operator $\mu\hat{q} + \nu\hat{p}$ for the eigenvalue X . For an arbitrary state with wave function $\Psi(y)$, the tomogram is expressed in terms of the fractional Fourier transform of the wave function:

$$\begin{aligned} M(X, \mu, \nu) &= \langle X, \mu, \nu | \Psi \rangle \langle \Psi | X, \mu, \nu \rangle \\ &= \frac{1}{2\pi|\nu|} \left| \int \Psi(y) \exp\left(\frac{i\mu}{2\nu}y^2 - \frac{iXy}{\nu}\right) dy \right|^2. \end{aligned} \quad (2)$$

In experiments with homodyne detection of photon states, an optical tomogram is measured. This tomogram reads

$$\begin{aligned} w(X, \theta) &= \text{Tr}[\hat{\rho}\delta(X - \hat{q}\cos\theta - \hat{p}\sin\theta)] \\ &= \langle X, \theta | \hat{\rho} | X, \theta \rangle, \end{aligned} \quad (3)$$

where $|X, \theta\rangle$ is an eigenvector of the Hermitian operator $\hat{q}\cos\theta + \hat{p}\sin\theta$ for the eigenvalue X .

The tomograms (1) and (3) are related:

$$\begin{aligned} w(X, \theta) &= M(X, \cos\theta, \sin\theta), \quad (4) \\ M(X, \mu, \nu) &= \frac{1}{\sqrt{\mu^2 + \nu^2}} w\left(\frac{X \text{sgn}(\nu)}{\sqrt{\mu^2 + \nu^2}}, \cot^{-1} \frac{\mu}{\nu}\right). \end{aligned} \quad (5)$$

The density operator can be reconstructed as [21]

$$\hat{\rho} = \frac{1}{2\pi} \int M(X, \mu, \nu) e^{i(X - \hat{q}\mu - \hat{p}\nu)} dX d\mu d\nu. \quad (6)$$

In view of (5), the density operator can be expressed in terms of the optical tomogram $w(X, \theta)$:

$$\hat{\rho} = \frac{1}{2\pi} \int_0^\pi d\theta \iint_{-\infty}^{+\infty} dX d\eta w(X, \theta) |\eta\rangle e^{i\eta(X - \hat{q}\cos\theta - \hat{p}\sin\theta)}. \quad (7)$$

The invertible relationship between the measurable tomograms and density operators provides the possibility of using the optical tomogram as a primary object containing complete information on the quantum state. In fact, in [22] the quantum-evolution equation and the energy-level equation have been written in explicit form for the optical tomogram. The quadrature statistics can be obtained from the optical tomogram:

$$\langle X^n \rangle(\theta) = \int X^n w(X, \theta) dX. \quad (8)$$

Photon-number statistics can also be obtained from the optical tomogram. In fact,

$$\langle \hat{q}^n \rangle = \int X^n w(X, \theta = 0) dX, \quad (9)$$

$$\langle \hat{p}^n \rangle = \int X^n w(X, \theta = \pi/2) dX. \quad (10)$$

The mean photon number reads

$$\langle \hat{n} \rangle = \frac{1}{2} \int X^2 [w(X, \theta = 0) + w(X, \theta = \pi/2)] dX - \frac{1}{2}. \quad (11)$$

The experimental tomograms must satisfy the uncertainty relations. In tomographic form this reads

$$\begin{aligned} &\left\{ \int X^2 w(X, \theta = 0) dX - \left[\int X w(X, \theta = 0) dX \right]^2 \right\} \\ &\times \left\{ \int X^2 w(X, \theta = \pi/2) dX \right. \\ &\left. - \left[\int X w(X, \theta = \pi/2) dX \right]^2 \right\} \geq \frac{1}{4}. \end{aligned} \quad (12)$$

For example, for a coherent state the product in this relation equals 1/4.

We point out that optical tomography provides the possibility of direct measurement of the purity of a photon quantum state [23].

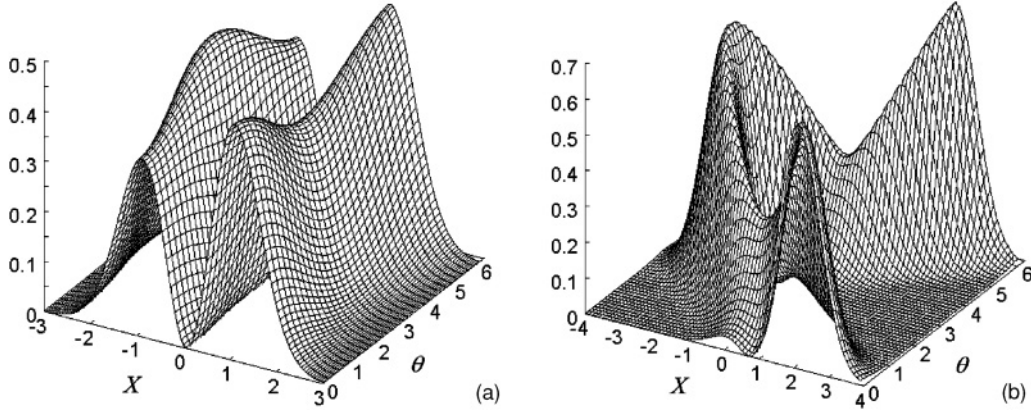


FIG. 1. Optical tomograms $w_\alpha(X, \theta)$ of photon-added coherent states for $\Omega(t) = 1$, $m = 1$, and $\alpha = 0.1$ (a) and $\alpha = 1$ (b).

III. OPTICAL TOMOGRAPHY OF PHOTON-ADDED STATES

A. Photon-added coherent states

Let us find the tomograms of the time-dependent photon-added coherent states $|\alpha, m, t\rangle$, studied in [3], of a one-mode parametric oscillator with the Hamiltonian

$$\hat{H} = \frac{\hat{p}^2}{2} + \Omega^2(t) \frac{\hat{q}^2}{2}, \quad \Omega(0) = 1.$$

The state $|\alpha, m, t\rangle$ is defined as follows:

$$\begin{aligned} |\alpha, m, t\rangle &= \hat{U}(t)|\alpha, m, 0\rangle = \hat{U}(t)|\alpha, m\rangle \\ &= [m!L_m(-|\alpha|^2)]^{-1/2} \hat{U}(t) \hat{a}^{+m} |\alpha\rangle, \end{aligned} \quad (13)$$

where $L_m(z) \equiv L_m^{(0)}(z)$ is the Laguerre polynomial [24,25], $|\alpha\rangle$ is the initial coherent state, and $\hat{U}(t)$ is the unitary evolution operator:

$$\hat{U}(t)\hat{U}^\dagger(t) = \hat{1}, \quad \hat{U}(0) = \hat{1}. \quad (14)$$

As shown in [3], the expression for the state $|\alpha, m, t\rangle$ in the coordinate representation has the form

$$\begin{aligned} M_{am}(X, \mu, \nu, t) &= \frac{[m!L_m(-|\alpha|^2)]^{-1}}{\sqrt{\pi}2^m |\dot{\varepsilon}\nu + \varepsilon\mu|} \left| H_m \left[\left(\frac{X\varepsilon + i\sqrt{2}\alpha\nu}{|\varepsilon|(\mu\varepsilon + \nu\dot{\varepsilon})} - \sqrt{\frac{\varepsilon^*}{2\varepsilon}}\alpha \right) \left(\frac{|\varepsilon|^2(\mu\varepsilon + \nu\dot{\varepsilon})}{\varepsilon^2(\mu\varepsilon^* + \nu\dot{\varepsilon}^*)} \right)^{1/2} \right] \right|^2 \\ &\times \left| \exp \left[-\frac{|\alpha|^2}{2} - \frac{X^2}{2|\mu\varepsilon + \nu\dot{\varepsilon}|^2} + \frac{\sqrt{2}\alpha X}{\mu\varepsilon + \nu\dot{\varepsilon}} - \frac{\alpha^2\varepsilon^*}{2\varepsilon} + \frac{i\nu\alpha^2}{\varepsilon(\mu\varepsilon + \nu\dot{\varepsilon})} \right] \right|^2. \end{aligned} \quad (19)$$

Substitution of $\mu = \cos\theta$ and $\nu = \sin\theta$ into (19) gives us, according to (4), the optical tomogram $w_{am}(X, \theta, t)$. In the case of a stationary Hamiltonian ($\Omega(t) = 1$, $\varepsilon = e^{it}$) we have

$$\begin{aligned} w_{am}(X, \theta, t, \Omega = 1) &= \frac{[m!L_m(-|\alpha|^2)]^{-1}}{\sqrt{\pi}2^m} \left| H_m \left(X - \frac{\alpha}{\sqrt{2}} e^{-i(t+\theta)} \right) \right|^2 \\ &\times \exp \left[-X^2 - |\alpha|^2 + 2\sqrt{2}X\text{Re}(\alpha e^{-i(t+\theta)}) - \text{Re}(\alpha^2 e^{-2i(t+\theta)}) \right]. \end{aligned} \quad (20)$$

$$\begin{aligned} \langle q|\alpha, m, t\rangle &= [m!L_m(-|\alpha|^2)]^{-1/2} \left(\frac{\varepsilon^*}{2\varepsilon} \right)^{m/2} \\ &\times H_m \left(\frac{q}{|\varepsilon|} - \sqrt{\frac{\varepsilon^*}{2\varepsilon}}\alpha \right) \langle q|\alpha, t\rangle, \end{aligned} \quad (15)$$

where $H_m(z)$ is the Hermite polynomial [24,25], $\langle q|\alpha, t\rangle$ is the time-dependent coherent state,

$$\langle q|\alpha, t\rangle = \pi^{-1/4} \varepsilon^{-1/2} \exp \left(\frac{i\dot{\varepsilon}q^2}{2\varepsilon} + \frac{\sqrt{2}\alpha q}{\varepsilon} - \frac{\alpha^2\varepsilon^*}{2\varepsilon} - \frac{|\alpha|^2}{2} \right), \quad (16)$$

which has been considered, e.g., in [26], and the c -number function $\varepsilon(t)$ satisfies the equation

$$\ddot{\varepsilon}(t) + \Omega^2(t)\varepsilon(t) = 0 \quad (17)$$

with the initial conditions $\varepsilon(0) = 1, \dot{\varepsilon}(0) = i$, which means that the Wronskian is

$$\varepsilon\dot{\varepsilon}^* - \varepsilon^*\dot{\varepsilon} = -2i. \quad (18)$$

The state $|\alpha, m, t\rangle$ is pure, so we can find the tomogram of it from Eq. (2). After some calculation we get

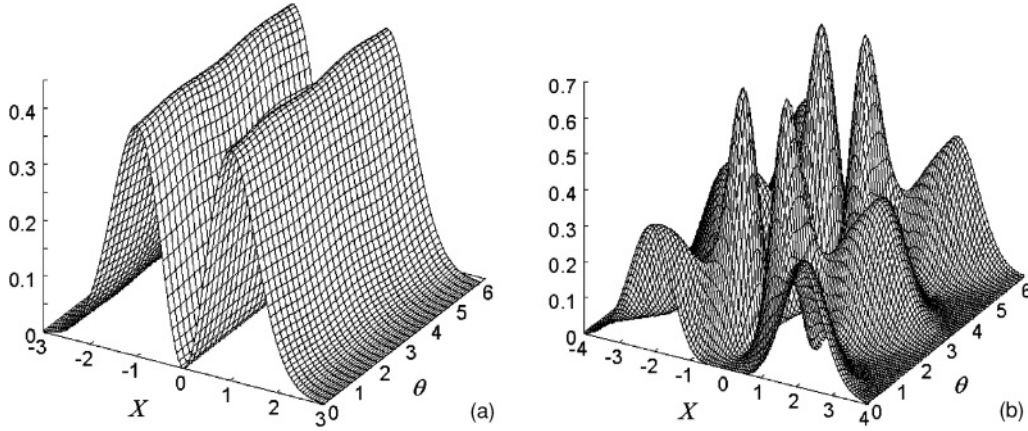


FIG. 2. Optical tomograms $w_{\alpha_{\pm}}(X, \theta)$ of even photon-added coherent states for $\Omega(t) = 1$, $m = 1$, and $\alpha = 0.1$ (a) and $\alpha = 1$ (b).

B. Photon-added even and odd coherent states

Photon-added even and odd coherent states $|\alpha_{\pm}, m\rangle$ were introduced in [4] as follows:

$$|\alpha_{\pm}, m\rangle = \frac{\hat{a}^{\dagger m} |\alpha_{\pm}\rangle}{(\langle \alpha_{\pm} | \hat{a}^m \hat{a}^{\dagger m} | \alpha_{\pm} \rangle)^{1/2}}, \quad (21)$$

where $|\alpha_{+}\rangle$ ($|\alpha_{-}\rangle$) is an even (odd) coherent state [19,27] and m is an integer. The normalized states $|\alpha_{\pm}\rangle$ can be written as

$$|\alpha_{+}\rangle = \frac{e^{|\alpha|^2/2}}{2\sqrt{\cosh|\alpha|^2}}(|\alpha\rangle + |-\alpha\rangle),$$

$$|\alpha_{-}\rangle = \frac{e^{|\alpha|^2/2}}{2\sqrt{\sinh|\alpha|^2}}(|\alpha\rangle - |-\alpha\rangle).$$

Photon-added even and odd coherent states $|\alpha_{\pm}, m\rangle$ can be represented in terms of photon-added coherent states $|\alpha, m\rangle$ as follows [4]:

$$|\alpha_{\pm}, m\rangle = \left\{ \frac{e^{|\alpha|^2} L_m(-|\alpha|^2)}{2[e^{|\alpha|^2} L_m(-|\alpha|^2) \pm e^{-|\alpha|^2} L_m(|\alpha|^2)]} \right\}^{1/2} \times (|\alpha, m\rangle \pm |-\alpha, m\rangle). \quad (22)$$

This equation, in view of (1) and (13), enables us to get the result

$$M_{\alpha_{\pm}m}(X, \mu, \nu, t) = \frac{e^{|\alpha|^2} L_m(-|\alpha|^2)}{2[e^{|\alpha|^2} L_m(-|\alpha|^2) \pm e^{-|\alpha|^2} L_m(|\alpha|^2)]} \times [M_{\alpha m}(X, \mu, \nu, t) + M_{-\alpha m}(X, \mu, \nu, t) \pm 2\text{Re}(\langle X, \mu, \nu | \alpha, m, t \rangle \langle -\alpha, m, t | X, \mu, \nu \rangle)]. \quad (23)$$

From (4) we have $w_{\alpha_{\pm}m}(X, \theta, t) = M_{\alpha_{\pm}m}(X, \mu = \cos \theta, \nu = \sin \theta, t)$, and in the case of a stationary Hamiltonian with $\Omega(t) = 1$ we have $w_{\alpha_{\pm}m}(X, \theta, t) = w_{\alpha_{\pm}m}(X, t + \theta)$.

C. Photon-added thermal states

A thermal state is the most classical state of light, formed by a statistical mixture of coherent states. The density operator of a thermal state has the form $\hat{\rho}_T = Z^{-1} e^{-\hat{H}/T}$, $Z = \text{Tr}(e^{-\hat{H}/T})$. The associated optical tomogram reads $w_T(X, \theta) = \frac{1}{\sqrt{2\pi\sigma^2}} e^{-X^2/2\sigma^2}$, where $\sigma^2 = \frac{1}{2} \coth \frac{1}{2T}$. The density matrix of

the photon-added thermal state in the representation of Fock states $|n, t\rangle$ is given by

$$\begin{aligned} \langle k, t | \hat{\rho}_{Tm} | n, t \rangle &= \langle k, t | \hat{a}^{\dagger m} \hat{\rho}_T \hat{a}^m | n, t \rangle \\ &= \delta_{kn} \frac{(1 - e^{-1/T})^{m+1}}{m!} \frac{n!}{(n-m)!} \\ &\times e^{-(n-m)/T}, \quad k, n \geq m. \end{aligned} \quad (24)$$

The symplectic tomogram of this state can be written as follows:

$$M_{Tm}(X, \mu, \nu, t) = \sum_{n=0}^{\infty} \langle n+m, t | \hat{\rho}_{Tm} | n+m, t \rangle |\langle X, \mu, \nu | n+m, t \rangle|^2. \quad (25)$$

Noting that $|\langle X, \mu, \nu | n, t \rangle|^2 = M_{\alpha=0, n}(X, \mu, \nu, t)$, with the help of (19) we find that

$$M_{Tm}(X, \mu, \nu, t) = \frac{(1 - e^{-1/T})^{m+1}}{\sqrt{\pi} m! 2^m |\mu\varepsilon + \nu\hat{\varepsilon}|} e^{-X^2/|\mu\varepsilon + \nu\hat{\varepsilon}|^2} \times \sum_{n=0}^{\infty} \frac{e^{-n/T}}{n! 2^n} \left| H_{n+m} \left\{ \frac{X\varepsilon}{|\varepsilon|(\mu\varepsilon + \nu\hat{\varepsilon})} \left[\frac{|\varepsilon|^2(\mu\varepsilon + \nu\hat{\varepsilon})}{\varepsilon^2(\mu\varepsilon^* + \nu\hat{\varepsilon}^*)} \right]^{1/2} \right\} \right|^2. \quad (26)$$

For the stationary Hamiltonian the optical tomogram reads

$$w_{Tm}(X, \theta) = \frac{(1 - e^{-1/T})^{m+1}}{\sqrt{\pi} m! 2^m} e^{-X^2} \sum_{n=0}^{\infty} \frac{e^{-n/T} H_{n+m}^2(X)}{n! 2^n}. \quad (27)$$

Thus the optical tomogram of the photon-added thermal state for the stationary Hamiltonian does not depend on time nor on the parameter θ . This equation, with the help of the known summing expression for Hermite polynomials [24],

$$\begin{aligned} (1 - \eta^2)^{-1/2} \exp \left[\frac{2xy\eta - (x^2 + y^2)\eta^2}{1 - \eta^2} \right] \\ = \sum_{n=0}^{\infty} \frac{H_n(x) H_n(y)}{2^n n!} \eta^n, \end{aligned} \quad (28)$$

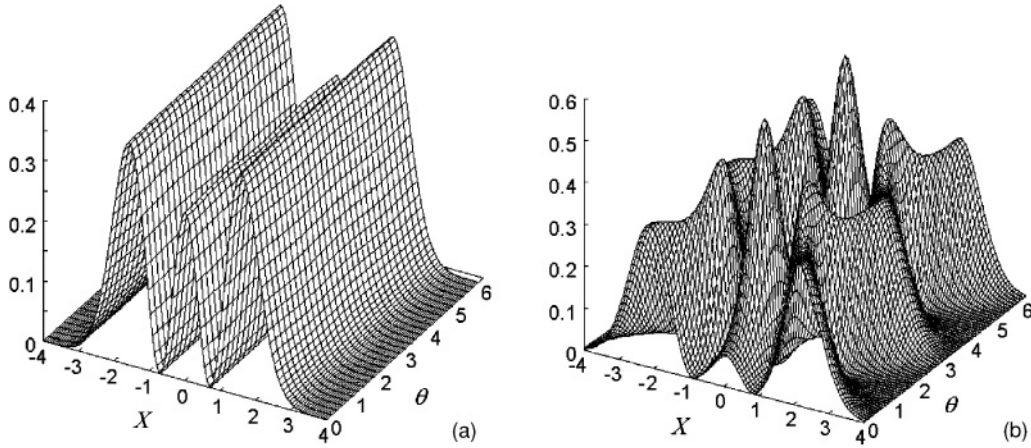


FIG. 3. Optical tomograms $w_{\alpha-}(X, \theta)$ of odd photon-added coherent states for $\Omega(t) = 1$, $m = 1$, and $\alpha = 0.1$ (a) and $\alpha = 1$ (b).

is transformed to the differential expression for $w_{Tm}(X, \theta) = w_{Tm}(X)$:

$$w_{Tm}(X) = \frac{(1 - e^{-1/T})^{m+1}}{\sqrt{\pi} m!} e^{-X^2} \frac{\partial^m}{\partial \eta^m} \left[\frac{\exp\left(\frac{2X^2 \eta}{1+\eta}\right)}{\sqrt{1-\eta^2}} \right]_{\eta=e^{-1/T}}. \quad (29)$$

This gives us, for $m = 1$ and $m = 2$, the following relations:

$$w_{Tm=1}(X) = \frac{(1 - e^{-1/T})^2}{\sqrt{\pi} \sqrt{1 - e^{-2/T}}} e^{-X^2 \tanh(1/2T)} \times \left[\frac{2X^2}{(1 + e^{-1/T})^2} + \frac{e^{-1/T}}{1 - e^{-2/T}} \right], \quad (30)$$

$$w_{Tm=2}(X) = \frac{(1 - e^{-1/T})^3}{2\sqrt{\pi} \sqrt{1 - e^{-2/T}}} e^{-X^2 \tanh(1/2T)} \times \left[\frac{4X^4}{(1 + e^{-1/T})^4} + \frac{4X^2(2e^{-1/T} - 1)}{(1 + e^{-1/T})^2(1 - e^{-2/T})} + \frac{2e^{-2/T} + 1}{(1 - e^{-2/T})^2} \right]. \quad (31)$$

In Figs. 1–4 we present tomograms of various sample photon-added states.

IV. CONCLUSION

In summary, we point out the main results of our paper. We have calculated the optical tomograms of photon-added states. The initial states to which the photons were added were chosen to be coherent states, even and odd coherent states, and thermal states. We considered these states because they have been achieved experimentally [7,8,10]. We pointed out that, in the probability representation of quantum mechanics, optical tomograms can be considered as primary objects containing complete information on quantum states (see, e.g., [15]).

In view of this, the reconstruction of the Wigner function or the Husimi function does not add extra information on the state. Thus the problem is to measure the optical tomogram with the highest possible accuracy. The precision of experiments for measuring optical tomograms can be checked using criteria such as the quadrature uncertainty relation with a purity (temperature)-dependent bound [28]. This criteria was suggested in [23] for controlling the precision of homodyne experiments. In the mentioned experimental works [7–11], including the homodyne two-mode studies [20], such checks have not been done. This is especially important, considering that the local-oscillator phase contribution can influence the

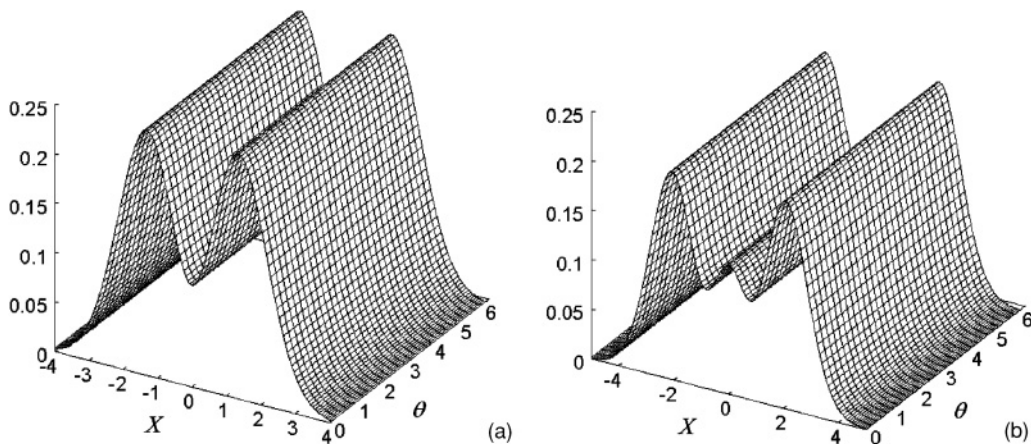


FIG. 4. Optical tomograms $w_{Tm}(X, \theta)$ of thermal states for $T = 1$ and $m = 1$ (a) and $m = 2$ (b).

final results if the states under study differ from the states (thermal or photon-added thermal) with optical tomograms that do not depend on the local-oscillator phase.

It is of special interest to test the experimental optical tomogram in the sense of satisfying the symmetry condition with respect to a shift of local-oscillator phase by π , as discussed in the introduction. In view of this we suggest accurately measuring the optical tomograms not only in the domain $0 \geq \theta \geq \pi$ of the local-oscillator phase, where the tomogram completely describes the quantum state, but in the domain $0 \geq \theta \geq 2\pi$, to check the symmetry properties of the tomogram.

Using theoretically calculated optical homodyne probabilities as a standard for comparison with experimental results, one can estimate the need for improvement in the precision of future experiments.

ACKNOWLEDGMENTS

V.I.M. thanks the Russian Foundation for Basic Research for partial support under Projects No. 09-02-00142 and No. 10-02-00312.

-
- [1] V. V. Dodonov, *J. Opt. B: Quantum Semiclass. Opt.* **4**, R1 (2002).
 - [2] G. S. Agarwal and K. Tara, *Phys. Rev. A* **43**, 492 (1991).
 - [3] V. V. Dodonov, M. A. Marchioli, Ya. A. Korennoy, V. I. Man'ko, and Y. A. Moukhin, *Phys. Rev. A* **58**, 4087 (1998).
 - [4] V. V. Dodonov, Ya. A. Korennoy, V. I. Man'ko, and Y. A. Moukhin, *J. Opt. B: Quantum Semiclass. Opt.* **8**, 413 (1996).
 - [5] A. V. Dodonov and S. S. Mizrahi, *Phys. Rev. A* **79**, 023821 (2009).
 - [6] V. V. Dodonov and S. S. Mizrahi, *J. Phys. A* **35**, 8847 (2002).
 - [7] A. Zavatta, S. Vicinai, and M. Bellini, *Science* **306**, 660 (2004).
 - [8] V. Parigi, A. Zavatta, M. Kim, S. Vicinai, and M. Bellini, *Science* **317**, 1890 (2007).
 - [9] M. Barbieri, N. Spagnolo, M. G. Genoni, F. Ferreyrol, R. Blandino, M. G. A. Paris, P. Grangier, and R. Tualle-Brouri, *Phys. Rev. A* **82**, 063833 (2010).
 - [10] A. Zavatta, V. Parigi, M. S. Kim, H. Jeong, and M. Bellini, *Phys. Rev. Lett.* **103**, 140406 (2009).
 - [11] T. Kiesel, W. Vogel, M. Bellini, and A. Zavatta, *Phys. Rev. A* **83**, 032116 (2011).
 - [12] D. T. Smithey, M. Beck, M. G. Raymer, and A. Faridani, *Phys. Rev. Lett.* **70**, 1244 (1993).
 - [13] A. I. Lvovsky and M. G. Raymer, *Rev. Mod. Phys.* **81**, 299 (2009).
 - [14] S. Mancini, V. I. Man'ko, and P. Tombesi, *Phys. Lett. A* **213**, 1 (1996).
 - [15] A. Ibort, V. I. Man'ko, G. Marmo, A. Simoni, and F. Ventriglia, *Phys. Scr.* **79**, 065013 (2009).
 - [16] D. Kalamidas, C. C. Gerry, and A. Benmoussa, *Phys. Lett. A* **372**, 1937 (2008).
 - [17] M. Aspelmeyer, S. Groblacher, K. Hammerer, and N. Kiesel, *J. Opt. Soc. Am. B* **27**, A189 (2010).
 - [18] S. Sivakumar, e-print [arXiv:1101.3855v1](https://arxiv.org/abs/1101.3855v1) [quant-ph].
 - [19] V. V. Dodonov, I. A. Malkin, and V. I. Man'ko, *Physica* **72**, 597 (1974).
 - [20] C. Eicher, D. Bozyigit, C. Lang, M. Baur, L. Steffen, J. M. Fink, S. Filipp, and A. Wallraff, e-print [arXiv:1101.2136v1](https://arxiv.org/abs/1101.2136v1) [quant-ph].
 - [21] G. M. D'Ariano, S. Mancini, V. I. Man'ko, and P. Tombesi, *J. Opt. B: Quantum Semiclass. Opt.* **8**, 1017 (1996).
 - [22] Ya. A. Korennoy and V. I. Man'ko, *J. Russ. Laser Res.* **32**, 74 (2011).
 - [23] V. I. Man'ko, G. Marmo, A. Porzio, S. Solimeno, and F. Ventriglia, *Phys. Scr.* **83**, 045001 (2011).
 - [24] Bateman Manuscript Project, *Higher Transcendental Functions*, edited by A. Erdélyi (McGraw-Hill, New York, 1953).
 - [25] G. Szegő, *Orthogonal Polynomials* (American Mathematical Society, Providence, 1959).
 - [26] I. A. Malkin and V. I. Man'ko, *Phys. Lett. A* **31**, 243 (1970).
 - [27] N. A. Ansari and V. I. Man'ko, *Phys. Rev. A* **50**, 1942 (1994).
 - [28] V. V. Dodonov and V. I. Man'ko, *Invariants and the Evolution of Nonstationary Quantum Systems, Proceedings of the Lebedev Physical Institute*, Vol. 183 (Nova Science, New York, 1989).